Advanced Journal of Chemistry-Section A, 2020, *3*, S750–S759 (*Special Issue*)
Available online at : www.ajchem-a.com
ISSN Online: 2645-5676
DOI: 10.22034/AJCA.2020.108183

Original Research Article

Development and Characterization of MWCNT/EPDM Based Composite as a Thermal Insulator for High Thermal Applications

Mahmoud Awad[a,*], Tamer Wafy[b]

[a] *Department of Chemical Engineering, Cairo University, Cairo, Egypt*
[b] *Department of Chemical Engineering, Military Technical College, Cairo, Egypt*

ARTICLE INFO

Received: 04 March 2020
Revised: 01 June 2020
Accepted: 04 June 2020
Available online: 08 June 2020

KEYWORDS

EPDM
MWCNT
Thermal characterization
Oxy- acetylene torch test
Ablation

ABSTRACT

Thermal insulators based on ethylene propylene diene terpolymer (EPDM) is an effective class of extreme temperature thermal insulators due to their outstanding heat, mechanical and ablative characteristics. This classed insulator is often reinforced by Kevlar pulp and fumed silica. Ammonium sulfate and antimony trioxide combination have been added as a flame retardant. To improve the elastomer ablative characteristics, multi-walled carbon nanotubes (MWCNTs) were added. We have studied different MWCNT concentrations. In this work, we investigated the effect of the MWCNTs content on the characteristics of the selected insulating formulation based on EPDM. The maximum improvement of tensile strength was 60%. Thermal stability increased by 27% through thermal gravimetric analysis (TGA-DTG), while the ablation resistivity was significantly increased by 60%. The weight loss of the 10 phr MWCNT sample decreased by 40% compared with that of the neat sample. Besides, an increase in ablation rate by 60% was recorded with the same sample.

GRAPHICAL ABSTRACT

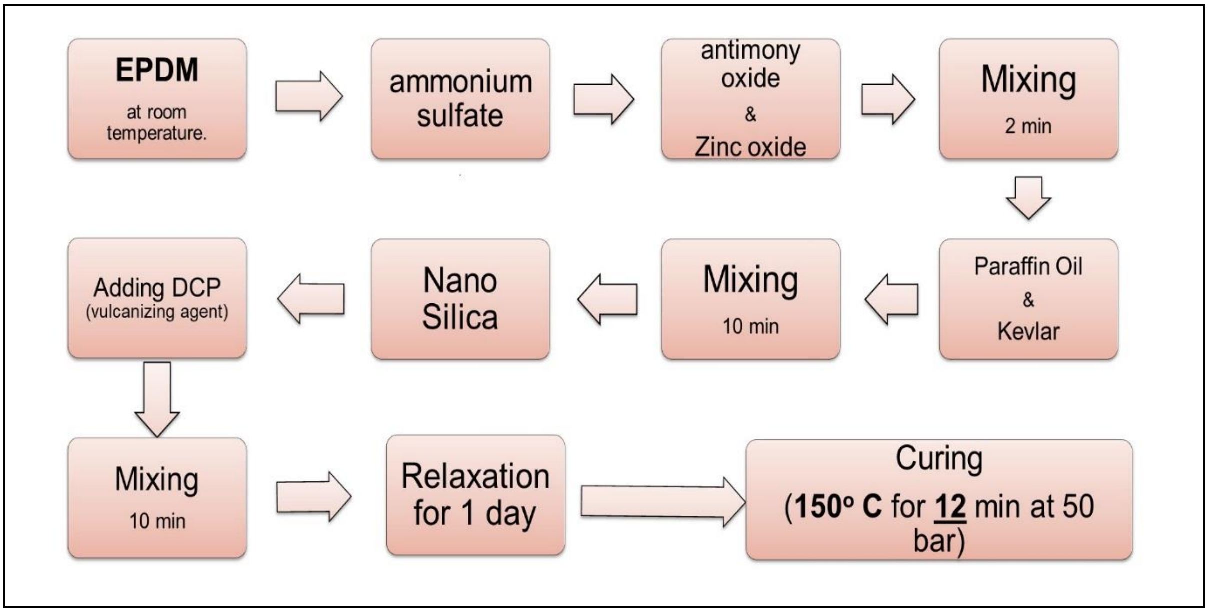

* Corresponding author's E-mail address: ma7mood.3emad@gmail.com

Introduction

An elastomeric thermal insulator for solid rocket motors (SRM) is found between the solid propellant and the motor chamber. There are two important functions for this elastomeric layer. First, it absorbs the mechanical stresses caused by the rocket motor during the casting the propellant, storage, and operation [1]. Second, it protects the motor case against high-temperature gases and particles produced by the propellant combustion, as passive cooling system [2,3]. It also protects the structures, aerodynamic surfaces, and vehicles and rockets' payload during ultrasonic flight through the atmosphere.

The external case of an SRM that serves as a combustion gas pressure vessel must be protected from high temperatures (above 2800 °C) generated from fuel combustion and accumulating pressures (around 60 bar). A phenomenon called ablation occurs to the insulating layer caused by the high flow rate of combustion gases emitting from SRM. It is an erosive process with material removal by combining thermo-mechanical and thermo-chemical conditions from elevated temperature, pressure, and combustion flame high velocities in SRM [3].

Ethylene-propylene diene terpolymer (EPDM) has great resistance to oxidation, weathering effects, and excellent low-temperature properties [4]. Also, EPDM has the lowest elastomer density (~0.85 g/cm^3) [5]. It has thermal conductivity and glass transition temperature of approximately 0.25 W/m/K and -50 °C respectively [6], which can be used as an appropriate heat insulator binder. There are also two significant characteristics of EPDM: long shelf life and outstanding low-temperature characteristics. In the meantime, EPDM's char yield and ablation resistance are comparatively low and needs to be improved with fillers.

The burnt matrix is comparatively weak among the different kinds of polymeric matrices used in ablatives [7], even when using a high char retention material. Various kinds of reinforcements can be added to the matrix to enhance the char retention phenomena. Typically used fibers are produced from carbon, mineral asbestos, and glass. There is also a very significant role for micron powdered fillers. However, there are several limitations associated with the traditional ablative composites, which are in a micron-scale. Even at the presence of fibrous reinforcements, the material may suffer from strong mechanical erosion. On the other side, it was a clear improvement in matrix reinforcement after approaching nanosized reinforcements. Composite materials produced with Nano reinforcements have resulted in a new level of ablation [8,9].

Mengfei *et al*. reported that, the MWCNTs is a promising filler for improving the elastomeric insulators' mechanical and ablative properties [10]. Fumed silica can play a very significant role in enhancing the matrix with low density and enhancing the thermal resistivity, as well [11]. Although not so long ago, as a result of excellent mechanical, thermal and ablative performance, asbestos was the best reinforcement for solid rocket motor insulation; however, as a result of its environmental pollution, asbestos was discarded [12]. In comparison, Kevlar has no ablative resistivity like asbestos-reinforced insulators. Fibers have been used with other fillers, such as flame retardants or char formers, to enhance ablative efficiency [13]. Ammonium polyphosphate has also been used as a char former and flame retardant in the latest years to reduce flame spread rates [14]. Ammonium sulfate and antimony oxide are also used as hybrid flame retardants [15]. A hybrid flame retardant blocks the surface of the composite when a carbonized layer is formed on the flame side.

Experimental

A low viscosity semi-crystalline grade ethylene-propylene-diene rubber (DuPont, Dutral TER-4049), locally supplied by El-kammash, Egypt supplier of Versalis Italy, was used as a matrix. Aramid pulp (commercial name: Twaron 1099,) was supplied by Teijin Co, China. Fumed nano-silica grade (Aldrich) was used to improve the ablation resistance of the material: according to the extensive literature previously reported on EPDM-based elastomeric thermal insulators, 15 phr of Nano silica resulted to be a proper amount of silica able to produce good ablative properties. Paraffin oil (BFR 20, provided by Alfa- Egypt) was used as a plasticizer: the use of oils decreases the mixing energy and time also improving the preservation of the fibrous reinforcements [16]. A crystalline dicumyl peroxide (Sigma Aldrich) was selected as a vulcanizing agent. The EPDM was prepared using a double rolls calendar. First, at room temperature, the raw EPDM was added to the calendars. Then Nano silica was then added then flame retardant, and Nano silica were added, respectively. Ten minutes of mixing was applied then Kevlar fiber and oil were added. Finally, the peroxide was added with 30 min of constant mixing.

The precise formulations of all compositions are reported in Table 1. Composite materials contain carbon nanotubes of specific weights. The compounds were vulcanized for 10 min at 180 °C in a 50-bar heated press, creating two-sheet kinds: one with a 2 mm thickness and the other with a 15 mm thickness. From the first type of sheet, samples of dog bones for mechanical analysis and cylindrical samples (50 mm diameter) used for the oxyacetylene torch experiment.

The thermal stability of the composites was investigated using a Thermogravimetric Analyzer (TGA) Q500 and consisted of dynamic scans with the Ramp technique at a heating rate of 20 °C/min. The samples were tested in nitrogen from room temperature to 1000 °C. Bulk samples of about 1-2 mg were used.

Testing ablative materials requires the use of hyperthermal environments with very high heat fluxes, conditions that cannot be generated through TG analysis, both in terms of the high heating rate (up to 50,000 °C/min) and because of the impossibility of simulating any shear stress induced by combustion gases. In this study, the extreme hyperthermal environment was simulated by an oxy-acetylene torch: this test setup is capable of producing both high temperatures (up to 3000 °C) [17] and elevated heat fluxes (up to 900 W/cm^2) [7]. This setup has effectively performed in many studies on ablatives: a more comprehensive description of this device can be discovered in Natali *et al.* [7].

Table 1. Compositions of the different formulations

	Neat	CN 0.5	CN 1	CN 2	CN 5	CN 10
EPDM (Phr)	100	100	100	100	100	100
Peroxide (Phr)	5	5	5	5	5	5
Paraffin oil (Phr)	4	4	4	4	4	4
Ammonium Sulphate (Phr)	35	35	35	3 5	35	35
Sb2O3 (Phr)	10	10	10	10	10	10
Kevlar pulp (Phr)	4	4	4	4	4	4
Fumed Silica (Phr)	15	15	15	15	15	15
Multi-walled Carbon nanotubes MWCNTs (Phr)	-	0.5	1	2	5	10

The test kit is built mainly from a 300 mm×300 mm×6 mm steel sheet with a 400× 300×8 mm horizontal wooden base. A high-temperature *k*-type thermocouple is attached to the steel sheet with high-temperature liner. The thermocouple can accurately read temperature up to 1200 °C. In this experiment, the distance between the sample surface and the flame was set at 10 mm and the torch heat flux was set at 500 W/cm^2. Acetylene by an oxidizer ratio equivalent to 1.33 has been chosen to create a neutral flame: this situation enables the thermo-oxidizing ablation of the tested material to be minimized to fulfill ASTM E-285-80 requirements [17]. On the steel sheet back-face, the temperature profile was acquired. All samples have been introduced to 40 s of flame [18]. The weight loss owing to the process of ablation was also calculated.

Results and discussion

Samples of carbon nanotubes were compared to each other and the neat sample as follows:

Thermogravimetric analysis

The TG (weight loss curves) and DTG (derivative weight loss) patterns of the compositions are shown in Figure 1 and Figure 3, respectively, while Figure 2 demonstrates a magnified zone of Figure 1.

Figure 1. TG results of MWCNTs/EPDM samples in nitrogen

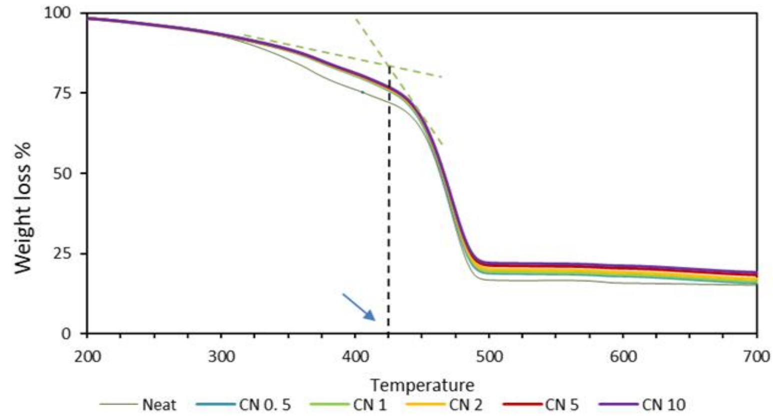

Figure 2. Magnified TG patterns at a specific range of temperature

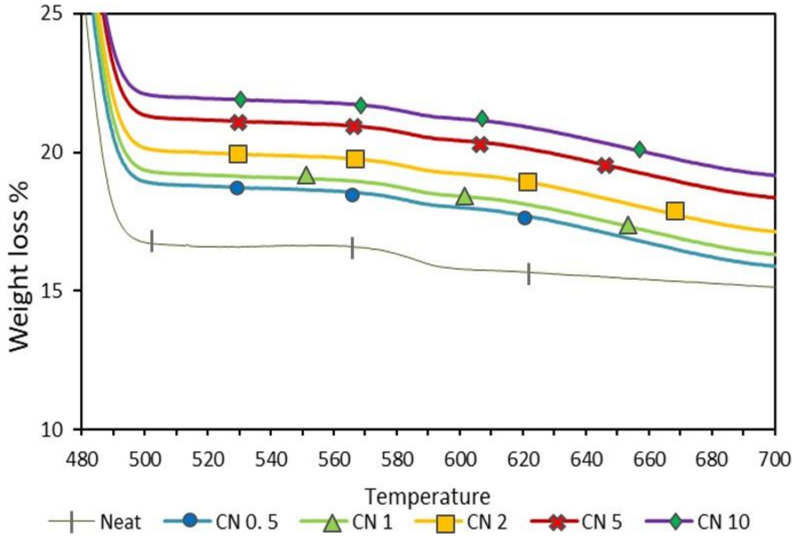

The TG results nearly have the same degradation pattern. The residue percentage differs slightly and illustrated in Table 2 at a final temperature of 700 °C. The onset temperature of these samples has been found close to 425 °C.

By increasing the carbon nanotubes content, the residue percentage increases that increased the thermal stability.

The DTG curves show that by increasing the MWCNTs percentage, the peak of DTG shifted to the right side, showing an increase in the temperature at which the maximum degradation rate occurs. Also, the peak of DTG analysis decreased by increasing the carbon content. Table 3 and Figure 4 state the peak values of the DTG curves to clarify the effect of MWCNT.

Table 2. Residues percentage after TG analysis at 700 °C composition neat

composition	Neat	CN 0.5	CN 1	CN 2	CN 5	CN 10
Residue %	15.1	15.88	16.31	17.14	18.36	19.17

Figure 3. DTG patterns of the produced elastomeric heat-shielding materials in nitrogen

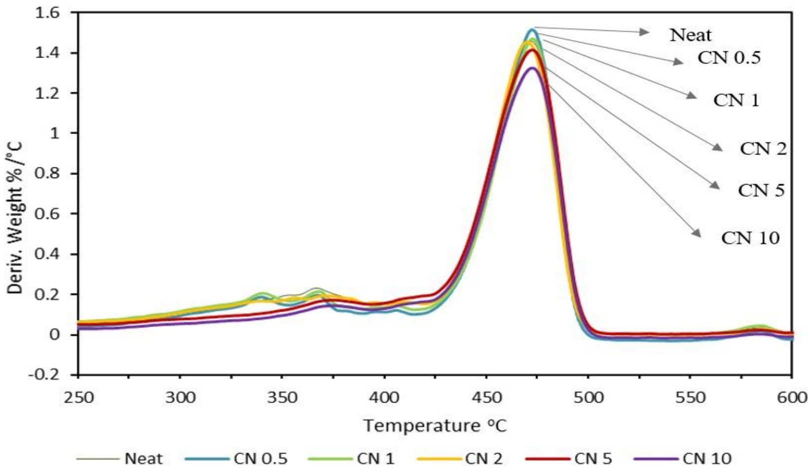

Table 3. Peak values of DTG analysis for MWCNTs samples

	Neat	CN 0.5	CN 1	CN 2	CN 5	CN 10
Temperature	471.35	472.72	472.96	470	472.47	472.49
Deriv. weight	1.46	1.51	1.47	1.454	1.415	1.325

Figure 4. Chart of Peak values of DTG analysis for MWCNTs samples.
Error for temperature (±0.5 °C) and (±1%) for derivative wt

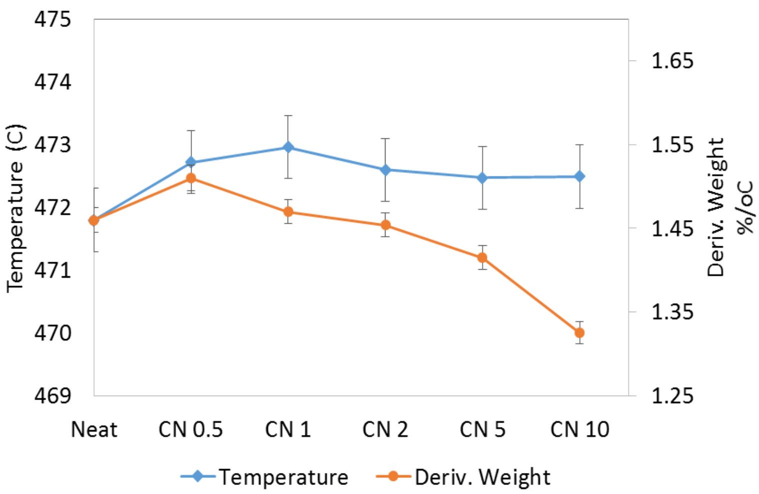

Thermomechanical analysis

The TMA patterns presented in Figure 5 illustrates the dimensional stability of the prepared carbon nanotubes containing samples. The samples were almost stable up to about 350 °C. Above this temperature, the dimensional stability is nearly proportional to the carbon nanotubes content. The calculated coefficients of thermal expansion (CTE) are presented in Figure 6.

As shown in Figure 5, more stability in dimensions change of CN 10 then stability decreased till neat sample. CTE of the CN 10 sample decreased by about 66% relative to the neat sample. Carbon nanotubes samples revealed lower CTE than carbon black samples, which means carbon nanotubes supply higher thermo-mechanical stability.

Mechanical and physical properties

Mechanical and physical properties were evaluated (Table 4). Increasing the carbon nanotubes percentage enhanced the density of matrix indeed. However, the density of sampled was still in an acceptable limit (<2 g/cm3). Hardness was measured using the REX-1600 shore-A device. It was found that, the hardness was increased by raising the carbon nanotubes content. As a result, by increasing the hardness, the resilience decreased. The introduction of MWCNTs to the samples increased the tensile strength and hardness. An increase in elongation at break of the samples appeared by increasing the MWCNT percentage.

Figure 5. TMA patterns for carbon nanotubes containing samples

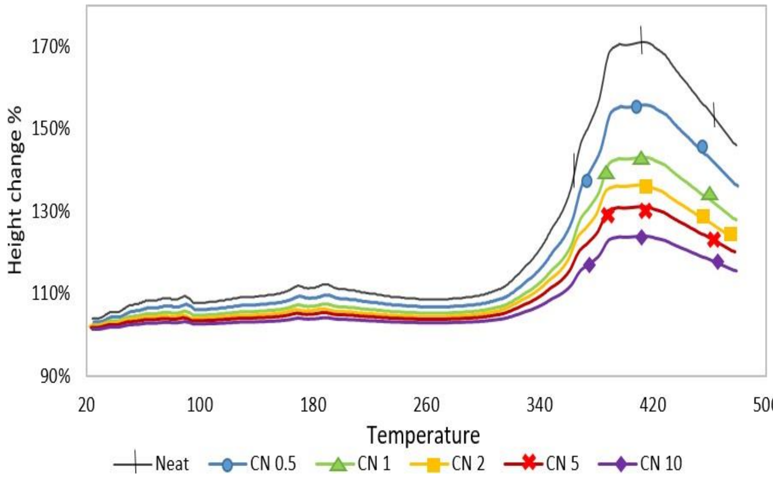

Figure 6. Thermal expansion coefficients for the MWCNT containing samples

Oxy-acetylene torch test results

Ablation properties were determined from the in-depth temperature profiles as recorded during the standard oxy-acetylene torch test and from the associated weight loss. As shown in Figure 7, a data logger (TECPEL 319) and data acquisition recorded the back-face temperature during the test using a *K*-type thermocouple (Figure 8). Recording temperature started from 15 s to allow the back face to warm up. The temperature recording ended at 40 s as the maximum time of flight of any rocket below 40 s.

Table 4. Mechanical and physical properties of tested sample property

	Neat	CN 0.5	CN 1	CN 2	CN 5	CN 10
Density (g/cm3)	1.8	1.801	1.803	1.808	1.811	1.821
Hardness (shore)	61	63	65	67	69	71
Resilience (%)	42.8	42.8	42.8	42.8	42.9	43
Tensile (MPa)	2.8	3.01	3.35	3.75	4.29	4.5
Elongation (%)	16.0	18.9	20.5	26.3	28.6	30.3

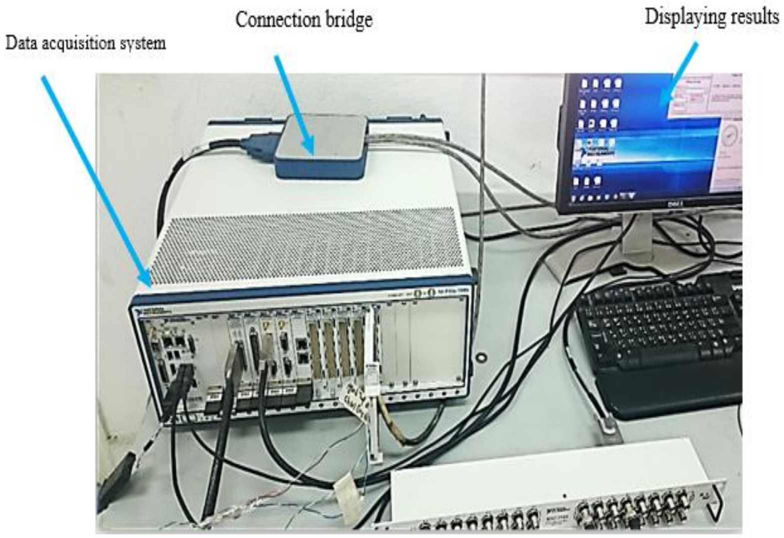

Figure 7. Data acquisition system connected with a data logger

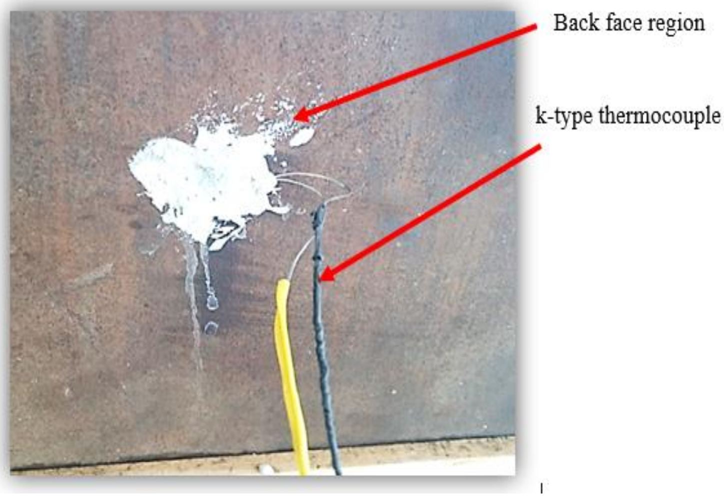

Figure 8. *K*-type thermocouple attached with thermally conductive cement

In-depth temperature profiles

After 15 s, a significant increase in the temperature profiles was observed. Figure 9 demonstrates that, by increasing the MWCNTs content, the temperature raised more rapidly. A maximum temperature of about 57 °C was recorded for the CN 10 sample. This increase in temperature was due to the high thermal conductivity of the nano-carbon. Table 5 present the results obtained from Figure 9.

Loss of weight

It is obvious that by increasing the carbon nanotubes content, the weight loss was improved. This improvement was basically due to the char layer formed by carbon content and the fire retardants. However, the improvement in weight loss percentage was insignificant. Also, the ablation rate decreased from 0.095 mm/s of the neat sample to 0.038 mm/s of the CN 10 sample. It is clear from these data that the weight loss is inversely proportional to MWCNT content. This is attributed to the formed char. The ablation rate as given in Table 6 exhibited also the same trend.

It is important to note that, the MWCNT samples formed a solid char layer as shown in Figure 10. This may be explained by the high tensile strength of MWCNTs which tends near 63 GPa [19]. These results were found to be in good agreement with the work conducted by Natali *et al.* [7]

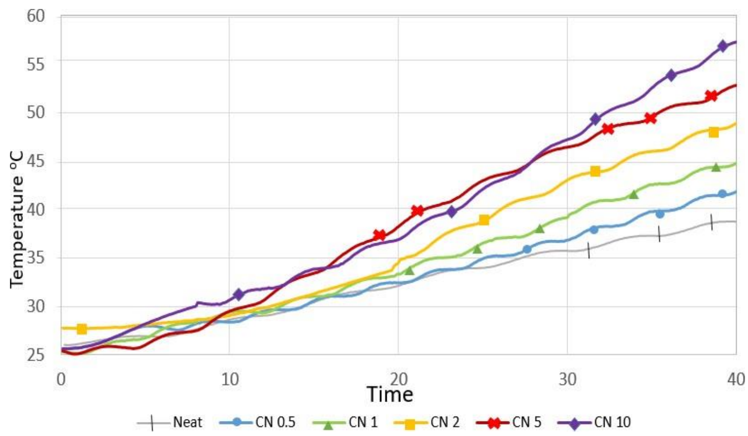

Figure 9. Oxy-acetylene torch test: Back-face temperature profile for the MWCNT containing samples

Table 5. Temperature of the back-face region at different duration

Time	Feedback temperature °C					
	Neat	CN 0.5	CN 1	CN 2	CN 5	CN 10
AT 15 (sec)	30.5	30.5	31.03	31.3	33.4	33.8
At 20 (Sec)	32.2	32.4	33.3	34.5	38.2	36.8
At 25 (Sec)	34.0	34.9	36.5	38.7	43	42.1
At 30 (Sec)	35.7	36.8	39.1	43	46.4	47.2
At 35 (Sec)	37.3	39.7	42.5	46	49.5	52.5
At 40 (Sec)	38.7	41.8	44.7	48.9	52.8	57.2

Table 6. Weight loss after ablation of CN samples

Sample	Neat		CN 0.5		CN 1		CN 2		CN 5		CN 10	
Weight	Before	After	Before	After	Before	After	Before	After	Before	After	Before	After
	12.3	11.21	12.5	11.62	13.63	12.7	12.06	11.3	11.8	11.1	12.2	11.5412
Weight loss %	8.86 %		7.02%		6.21%		6.01%		5.41%		5.40%	
Ablation rate (mm/s)	0.0951		0.089		0.078		0.053		0.045		0.038	

Figure 10. CN 10 sample after ablation test

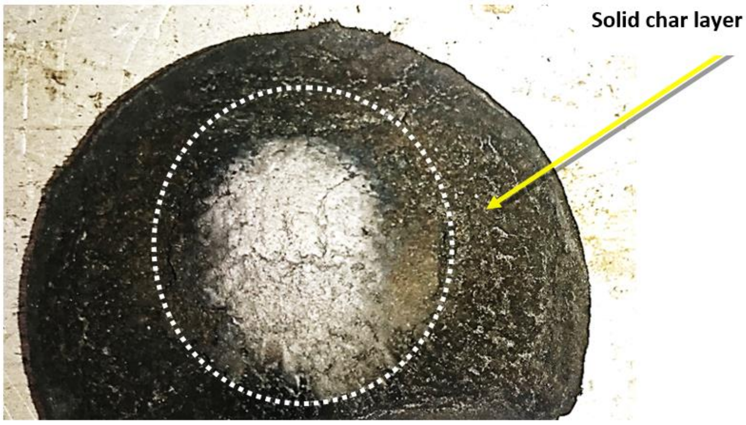

Conclusion

In this research study, the effect of carbon nanotubes content on the properties of a selected EPDM based insulating formulation has been investigated.

- The tensile strength of the CN10 sample was improved by 60%. Elongation was improved by 90%.
- The thermal stability also was slightly improved. The residue formation of CN 10 increased by 27% from the neat sample.
- The thermal expansion coefficient decreased from 1012 μm/m °C of the neat sample to 342.8 μm/m °C of CN 10 sample, which is an excellent improvement of thermo-mechanical properties.
- For the oxy-acetylene torch test, the back-face temperature of the samples increased; however, within the acceptable range for both sample types. The ablation resistance was considerably improved. The weight loss from CN 10 decreased by 39% relative to the neat sample. Also, the ablation rate was decreased by 60% for CN 10, which improved the ablation resistivity.
- The ablation rate of the CN 10 sample was 0.038 mm/s. MWCNT samples formed a solid char layer. This can be the cause of the 26% reduction of the ablation rate of MWCNT samples.
- The overall conclusion can be briefed as: the carbon nanotubes increased the mechanical and thermal properties and improve the ablative resistance properties of EPDM-based elastomers.
- These properties at the laboratory level showed that, the EPDM based MWCNTs nanocomposite systems are a promising composite which performed well for rocket motor insulation application compared to currently used insulations. Also, CN 10 is showing the best thermal, ablation performance compared to the other samples.

Acknowledgment

The authors are grateful to the University of Military Technical College, Egypt for its support.

Disclosure statement

No potential conflict of interest was reported by the authors.

ORCID

Mahmoud Awad : 0000-0003-2861-3813

References

[1] A.F. Ahmed, S.V. Hoa, *J. Compos. Mater.*, **2012**, *46*, 1549–1559.

[2] M. Mohamed, S. El-Marsafy, S. Hasanin, T. Wafy, *Int. Conference Aerospace Sci. Aviat. Technol.*, **2017**, *17*, 1–11.

[3] M.E. Awad, M. Nasser, *Adv. J. Chem. A*, **2020**, *3*, 370–377.

[4] M. Natali, I. Puri, M. Rallini, J. Kenny, L. Torre, *Computat. Mater. Sci.,* **2016**, *111*, 460–480.

[5] L.M.S. Murakami, M.F. Diniz, L.M. Silva, N.B. Sanches, R. D.C.L. Dutra, *Polym. Test.*, **2019**, *79*, 106042.

[6] M. Shi, D. Zhang, J. Zhu, Y. Shi, J. Sun, Y. Ji, *J. Thermoplast. Compos. Mater.,* **2019**, *32*, 922–935.

[7] M. Natali, M. Monti, D. Puglia, J.M. Kenny, L. Torre, *Compos. A Appl. Sci. Manufact.,* **2012**, *43*, 174–182.

[8] H. Ebadi-dehaghani, M. Nazempour, *Smart Nanoparticl. Technol.*, **2012**, 519-534.

[9] S. Singh, P. Guchhait, *Am. J. Macromol. Sci.*, **2014**, *1*, 1–16.

[10] M. Guo, J. Li, K. Xi, Y. Liu, J. Ji, *Acta Astronaut.,* **2019**, *159*, 508–516.

[11] Z. Xu, S. Zheng, X. Wu, Z. Liu, R. Bao, W. Yang, M. Yang, *Compos. Part A Appl. Sci. Manuf.*, **2019,** *125*, 105527.

[12] N. Joshi, S. Watanabe, R. Verma, R.P. Jablonski, C.I. Chen, P. Cheresh, N.S. Markov, P.A. Reyfman, A.C. McQuattie-Pimentel, L. Sichizya, Z. Lu, R. Piseaux-Aillon, D. Kirchenbuechler, A.S. Flozak, C.J. Gottardi, C.M. Cuda, H.Perlman, M. Jain, D.W. Kamp, G.R.S. Budinger, A.V. Misharin, *Eur. Respir. J.,* **2020**, *55*, 1900646.

[13] B.L. Zha, Y.A. Shi, J.J. Wang, Q.D. Su, *Study on ablation behavior of silicone rubber based insulation material under the condition of boron oxide particles erosion*. In IOP Conference Series: Materials Science and Engineering, IOP Publishing, **2018,** p 012003.

[14] P. Khalili, X. Liu, K.Y. Tshai, C. Rudd, X. Yi, I. Kong, *Composit. B Eng.*, **2019**, *159*, 165–172.

[15] T. Farajpour, Y. Bayat, M. Abdollahi, M.H. Keshavarz, *J. Appl. Polym. Sci.,* **2015**, *132*, 1–10.

[16] L. Liu, Z. Fang, A. Gu, Z. Guo, *Tribol. Lett.*, **2011**, *42*, 59–65.

[17] E. ASTM, Standard test method for oxyacetylene ablation testing of thermal insulation materials, *Annual Book of ASTM Standards*, **2008**, *15*, 1–6.

[18] M. Natali, M. Rallini, D. Puglia, J. Kenny, L. Torre, *Polym. Degradat. Stability*, **2013**, *98*, 2131–2139.

[19] H.I. Kim, M. Wang, S.K. Lee, J. Kang, J.D. Nam, L. Ci, J. Suhr, *Sci. Rep.*, **2017**, *7*, 1–7.

How to cite this manuscript: Mahmoud Awad, Tamer Wafy. Development and Characterization of MWCNT/EPDM Based Composite as a Thermal Insulator for High Thermal Applications, *Adv. J. Chem. A*, **2020**, *3*, S750–S759.